JOURNAL OF EXPERIMENTAL AND THEORETICAL PHYSICS, 2024, Vol. 165, No. 6, pp. 797–809

NUCLEI, PARTICLES, FIELDS, GRAVITY AND ASTROPHYSICS

POLARIZATION PROPERTIES OF BLACK HOLES AND WORMHOLES

© 2024 S. V. Chernov

Astro Space Center, Lebedev Physical Institute of the Russian Academy of Sciences 117997, Moscow, Russia
e-mail: chernov@lpi.ru

Received December 29, 2023
Revised December 29, 2023
Accepted January 23, 2024

Abstract. In this paper, using the example of the Lamy metric, the polarization properties of black holes and wormholes are investigated. Maps of linear polarization and the position of the angle of the electric vector are constructed for the toroidal and radial distribution of the magnetic field in thin disks. Using these results from future RSDB observations on the next-generation Event Horizon telescope and the Millimetron spacemission, it will be possible to determine whether the source is a black hole or a wormhole.

Keywords: *black hole, wormhole, linear polarization, lamy's metric*

DOI: 10.31857/S004445102406e051

1. INTRODUCTION

The Event Horizon Telescope (EHT) obtained an image of hot magnetized plasma emitting synchrotron radiation around supermassive black holes in the elliptical galaxy M87 [1] and in our Milky Way galaxy [2]. The images form a ring-like morphology and were obtained in the millimeter range at 230 GHz. However, intensity maps carry significantly less information than polarization maps. Because of this, it is not possible to constrain numerical models and determine plasma and black hole parameters from observations [3]. In 2021, based on EHT data, a linear polarization map of the supermassive black hole in M87* was published, revealing a spiral structure of the electric vector position angle in hot magnetized plasma [4]. The polarization map of M87* strongly constrained numerical models; in particular, it was found that the accretion flow structure is better described by the magnetically arrested disk (MAD) regime than by the standard and normal evolution (SANE) disk [5]. Therefore, polarimetric observations are a critically important step towards understanding physical processes in strong gravitational fields.

Another question that arises here is whether the image obtained in the EHT observations is actually an image of a black hole or an image of another object, such as a wormhole? To answer this question, a criterion for distinguishing between a black hole and a wormhole is needed. In this work, it is assumed that a black hole can be distinguished from a wormhole by linear polarization of radiation.

To construct polarization maps, it is necessary to calculate the polarization change along the photon trajectory. As known, radiation polarization can change for two reasons. The first is due to the rotation of the electric vector along the geodesic in strongly curved spacetime. The second is due to photon propagation in magnetized plasma. Here we will investigate the first reason. The strongly curved spacetime will be created either by a black hole or a wormhole.

In this article, using the Lamy metric as an example, the change in the linear polarization vector during photon motion in a strong gravitational field is calculated for both a black hole and a wormhole. For this purpose, a metric is chosen that describes both black holes and wormholes and in the limiting case coincides with the Kerr rotating black hole

metric. Maps of linear polarization and electric vector angle position depending on the magnetic field direction in a thin disk are constructed. Toroidal and radial magnetic field distributions in thin disks are considered. The decomposition coefficient β_2 of linear polarization depending on metric parameters is calculated and a criterion for distinguishing a black hole from a wormhole is given.

The paper uses a system of units in which the speed of light and gravitational constant are equal to unity, $c = G = 1$. The dimension of length is Gm/c^2, the dimension of time is Gm/c^3, where m is the mass parameter.

2. PHOTON EQUATIONS OF MOTION

In this section, we briefly describe the basic equations for light ray propagation in curved spacetime using the Lamy metric as an example.

The Lamy metric in Boyer-Lindquist coordinates (t, r, θ, φ) has the form [6]

$$ds^2 = -\left(1 - \frac{2rM(r)}{\Sigma}\right)dt^2 + \frac{\Sigma}{\Delta}dr^2 + \Sigma d\theta^2 + \frac{\sin^2\theta}{\Sigma}\left((r^2 + a^2)^2 - \Delta a^2 \sin^2\theta\right)d\varphi^2 - \frac{4raM(r)\sin^2\theta}{\Sigma}dtd\varphi, \quad (1)$$

where standard notations are introduced

$$\Sigma = r^2 + a^2\cos^2\theta,$$

$$\Delta = r^2 - 2rM(r) + a^2,$$

a — rotation parameter, spin. This metric differs from the Kerr rotating black hole metric in that the mass parameter M is not a constant value but is a function of the radial coordinate of the form [6]

$$M(r) = m\frac{|r|^3}{|r|^3 + 2mb^2}. \quad (2)$$

In this case, the parameter m is a constant value and we will call it the mass parameter, and the parameter b, as shown in work [7], is the magnetic charge. In the case when the magnetic charge is zero, $b = 0$, this metric coincides with the Kerr rotating black hole metric. Without loss of generality, we will assume that the mass parameter equals one, one, $m = 1$. Also in this work, we will consider the case when the magnetic charge takes values from zero to two, $0 \leqslant b \leqslant 2$. As shown in work [6], this manifold is geodesically complete and non-singular in all spacetime $-\infty < r < \infty$. This means that two asymptotically flat spacetimes are connected at the point $r = 0$. From expression (2), one can see that the value $M(r) \geqslant 0$ is always greater than or equal to zero for any radius, $-\infty < r < \infty$.

The Lamy metric has coordinate singularities that correspond to event horizons in the case of the Kerr metric. These conditions are determined by the expression of the form

$$\Delta = r^2 - 2rM(r) + a^2 = 0.$$

In the case when both parameters a and b are not equal to zero, equation $\Delta = 0$ is solved numerically. Figure 4 of article [6] shows cases when this equation either has no roots, or has one (extreme case) or two roots. These roots of equation $\Delta = 0$ will be called event horizons by analogy with the roots of the equation in the Kerr metric. If the Lamy metric has two or one event horizon, then this metric corresponds to a black hole metric, otherwise it corresponds to a wormhole.

Photons propagate in the Lamy metric, moving along geodesics described by equations of the form

$$\frac{dx^\alpha}{d\tau} = p^\alpha, \qquad \frac{dp^\alpha}{d\tau} = -\Gamma^\alpha_{\beta\gamma}x^\beta x^\gamma, \quad (3)$$

where $\Gamma^\alpha_{\beta\gamma}$ are Christoffel symbols, p^α is the photon momentum, τ is the affine parameter. Paper [8] presents metric coefficients and Christoffel symbols for the Lamy metric (1) with function form (2). Below we will show images of black holes and wormholes obtained through numerical solution of eight equations (3). Qualitatively, photon propagation in the Lamy metric, by analogy with the Kerr metric, can be described using radial and angular potentials of the form [3]

$$R(r) = (r^2 + a^2 - aL)^2 - \Delta\left(Q + (L - a)^2\right), \quad (4)$$

$$Q(\theta) = Q + \cos^2\theta\left(a^2 - \frac{L^2}{\sin^2\theta}\right), \quad (5)$$

where L is the angular momentum of the photon, Q is Carter's constant. In the Kerr metric ($b = 0$) dial potential is a fourth-order polynomial with respect to the radial coordinate. In the Lamy metric, this potential is a seventh-order polynomial [6] and, as shown in work [6], some photon trajectories can have more than one radial turning point.

To determine the position of the image on the observer's screen, Cartesian coordinates (α, β) are introduced, first presented in work [9]. These coordinates connect the conserved photon parameters (L, Q) with the position on the observer's screen:

$$a = -\frac{L}{\sin\theta_o}, \quad b = \pm\sqrt{Q(\theta_o)}, \quad (6)$$

where θ_0 is the observer's inclination angle to the rotation axis of the black hole or wormhole. Thus, knowing the photon's position on the observer's screen, one can determine the photon parameters (L, Q), and consequently, the position of the photon source in the disk.

To construct polarization maps, we will primarily be interested in photon polarization. To calculate the polarization change of a photon moving in a strong gravitational field, we will use the Walker-Penrose constants [10]. For this, we need to show that the Lami metric belongs to type D according to Petrov classification [10]. To demonstrate this, we will use the Newman-Penrose formalism. This formalism is a tetrad formalism in an isotropic basis consisting of four isotropic vectors (l, n, m, m*) [10]. The Appendix defines a quartet of isotropic vectors satisfying orthogonality conditions, isotropy, and normalization condition. The Ricci rotation coefficients in the Lami metric, which in this formalism are called spin coefficients [10], are also written out. Since the spin coefficients in the Lami metric

$$\kappa = \sigma = \lambda = \nu = \varepsilon = 0 \quad (7)$$

are equal to zero (see Appendix), from the corollary of the Goldberg-Sachs theorem, it follows that the Lami metric belongs to type D according to Petrov classification [10]. The Appendix also lists the non-zero Weyl scalar Ψ_2. All these quantities will be needed to calculate the Walker-Penrose constants.

We proceed to calculate the change in the photon polarization vector when moving in curved spacetime [10]. Let f^μ – 4-vector be the photon polarization, which is orthogonal to the photon 4-momentum p^μ, i.e.,

$$f^\mu p_\mu = 0,$$

and is parallel transported along the photon trajectory, i.e.,

$$p^\mu \nabla_\mu f^\nu = 0.$$

Then the quantity

$$K_s = -p^i f^j (l_i n_j - l_j n_i - m_i m_j^* + m_i^* m_j)\Psi_2^{-1/3} \quad (8)$$

remains constant along the geodesic [10]. The quantity

$$K_s = K_2 + iK_1$$

is a constant complex value called the Walker-Penrose constant. The existence of this constant allows us to calculate the change in the 4-vector of polarization along the photon trajectory and compare polarization values for black hole and wormhole metric cases. For this, we need to relate the quantities f and p near the observer and the source. We introduce the notations

$$A = p^t f^r - p^r f^t + a\sin^2\theta(p^r f^\theta - p^\theta f^r), \quad (9)$$

$$B = \sin\theta[(p^\theta f^\varphi - p^\varphi f^\theta)(r^2 + a^2) - a(p^t f^\varphi - p^\varphi f^t)]. \quad (10)$$

Then expression (8) can be rewritten as

$$K_2 + iK_1 = -(A - iB)\Psi_2^{-1/3}. \quad (11)$$

The values of 4-momentum at any point in spacetime are given in the Appendix by formulas (38). By setting the initial magnetic field at the emission point and calculating the constants K_1 and K_2, one can determine the values of the polarization 4-vector at

the observation point, and consequently, the Stokes parameters (see (53) and (54)).

Another important quantity is the linear polarization decomposition coefficient β_m, introduced in [11]:

$$b_m = \frac{1}{I_{ann}} \int_{r_{min}}^{r_{max}} \int_0^{2\pi} P(r,\varphi) P_m^*(\varphi) r\, dr\, d\varphi =$$

$$= \frac{1}{I_{ann}} \int_{r_{min}}^{r_{max}} \int_0^{2\pi} P(r,\varphi) e^{-im\varphi} r\, dr\, d\varphi, \qquad (12)$$

where

$$I_{ann} = \int_{r_{min}}^{r_{max}} \int_0^{2\pi} I(r,\varphi) r\, dr\, d\varphi, \qquad (13)$$

$$P(r,\varphi) = Q(r,\varphi) + iU(r,\varphi). \qquad (14)$$

Here Q and U are the Stokes parameters of linear polarization, (r,φ) are polar coordinates on the observer's screen, the asterisk "*" denotes complex conjugation, is the radiation intensity. Without loss of generality, we set the value I_{ann} equal to one, $I_{ann} = 1$. Let us denote the total linear polarization as

$$LP = \sqrt{Q^2 + U^2},$$

and the electric vector angle positions as

$$EVPA = \frac{1}{2} arctg \frac{U}{Q}. \qquad (15)$$

In the next section, we will present maps of total linear polarization and electric vector angle positions for radial and toroidal magnetic fields in a thin disk located in the equatorial plane of a black hole or wormhole, and compare the obtained results.

3. RESULTS

In this section, we will discuss the difference in maps of linear polarization and electric vector angle positions for a black hole and wormhole using the Lamy metric as an example.

We will assume that the source of photon radiation is a thin disk located in the equatorial plane of the black hole (wormhole), which radiates isotropically in all directions. The thin disk is penetrated by a radial or toroidal magnetic field. The inner radius of the disk was set to $r_{in} = 8$.. The rotation parameter in the Lamy metric was set to $a = 0.9$, and the magnetic charge to $b = 0, 0.3, 0.5, 0.7, 0.9, 2.0$. The case when $b \leq 0.245$ corresponds to a black hole, and the case when $b < 0.245$ to a wormhole (see Fig. 4 from [6]). The value 0.245 is determined numerically from the equation $\Delta = 0$ for spin $a = 0.9$. The observer is located at a distance from the black hole (wormhole) $r_o = 50$ at an angle $i = 17^\circ, 45^\circ, 80^\circ$ to the rotation axis of the black hole (wormhole). To construct polarization maps, the ray-tracing method was used. The geodesic equations (3) were solved numerically using the fourth-order Runge-Kutta method. All polarization maps are shown on a scale from -10 to 10 in units of Gm / c^2 and with a resolution of 2500×2500 pixels. The intensity images for the same metric parameters are shown in Fig. 3 of paper [8].

Figure 1 and 2 show linear polarization maps for the initial distribution of radial and toroidal magnetic fields, respectively. The color indicates the magnitude of linear polarization, LP value. Green arrows show the direction of the electric vector of linear polarization. The arrow length is proportional to the magnitude of linear polarization. The top three figures correspond to a black hole, the rest to a wormhole. The figures from left to right are for different inclination angles of the observer relative to the rotation axis of the black hole (wormhole), $i = 17°, 45°, 80°$. The figures from top to bottom are for different magnetic charge values, $b = 0, 0.3, 0.5, 0.7, 0.9, 2.0$.

Comparing linear polarization for black holes and wormholes, the following conclusions can be drawn. Linear polarization in photon rings for wormholes has higher values than in the disk. This is because for some photons, circular orbits are located closer to the center and, consequently, the gravitational field will much more strongly curve the trajectory of motion, and hence the magnitude of linear polarization. This statement is true for both radial and toroidal distributions of the magnetic field in the disk. The directions of linear polarization (shown by green arrows in the figures) in photon rings will be approximately perpendicular to each other for radial and toroidal magnetic fields when the observer is

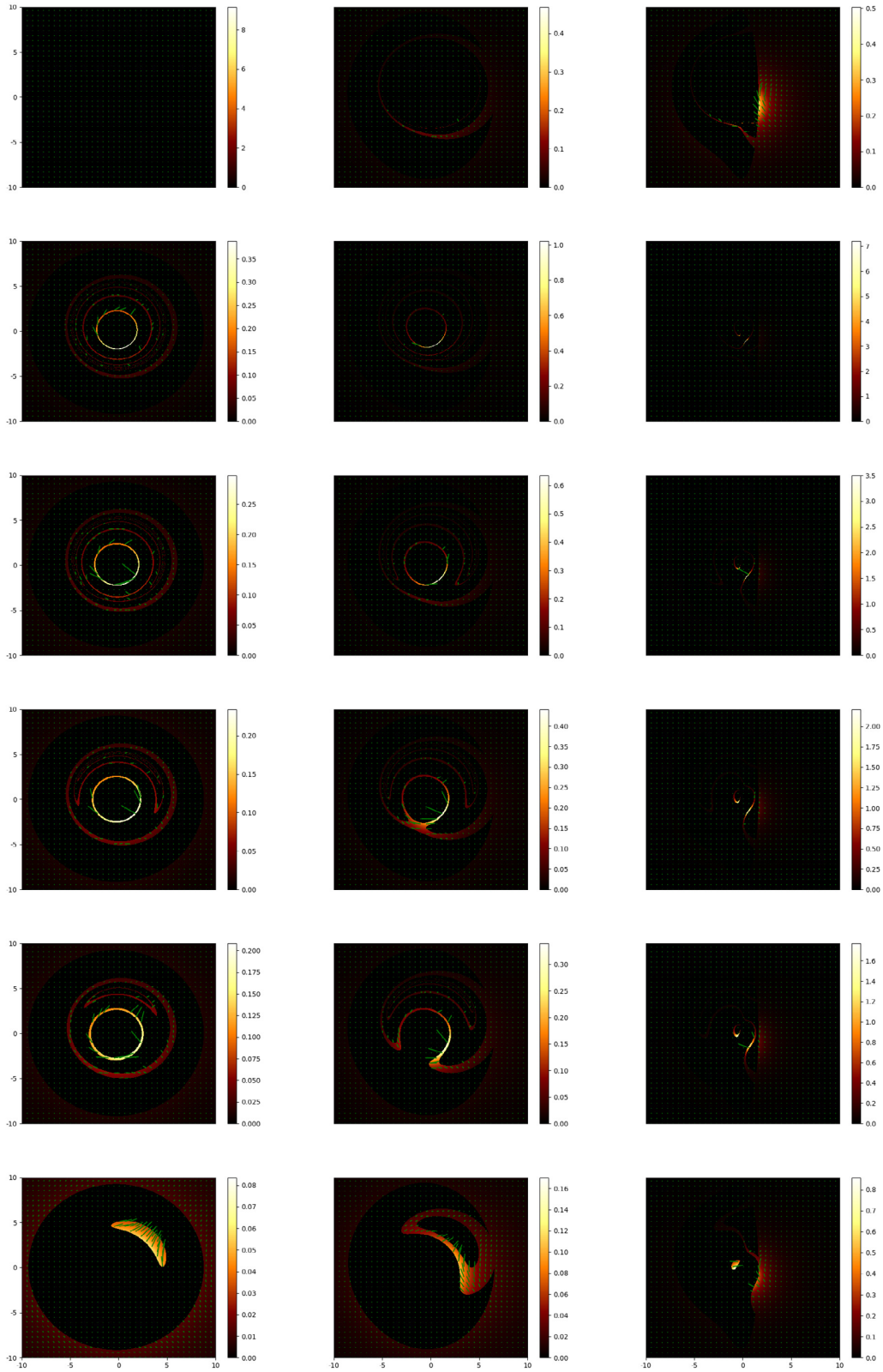

Fig. 1. Map of total linear polarization (shown in color) LP for the initial radial distribution of magnetic field around a black hole and wormhole. From left to right, inclination angles are $i = 17^\circ, 45^\circ, 80^\circ$. From top to bottom, magnetic charge is $b = 0, 0.3, 0.5, 0.7, 0.9, 2.0$. Map scale to -10Gm/c^3 to 10Gm/c^3

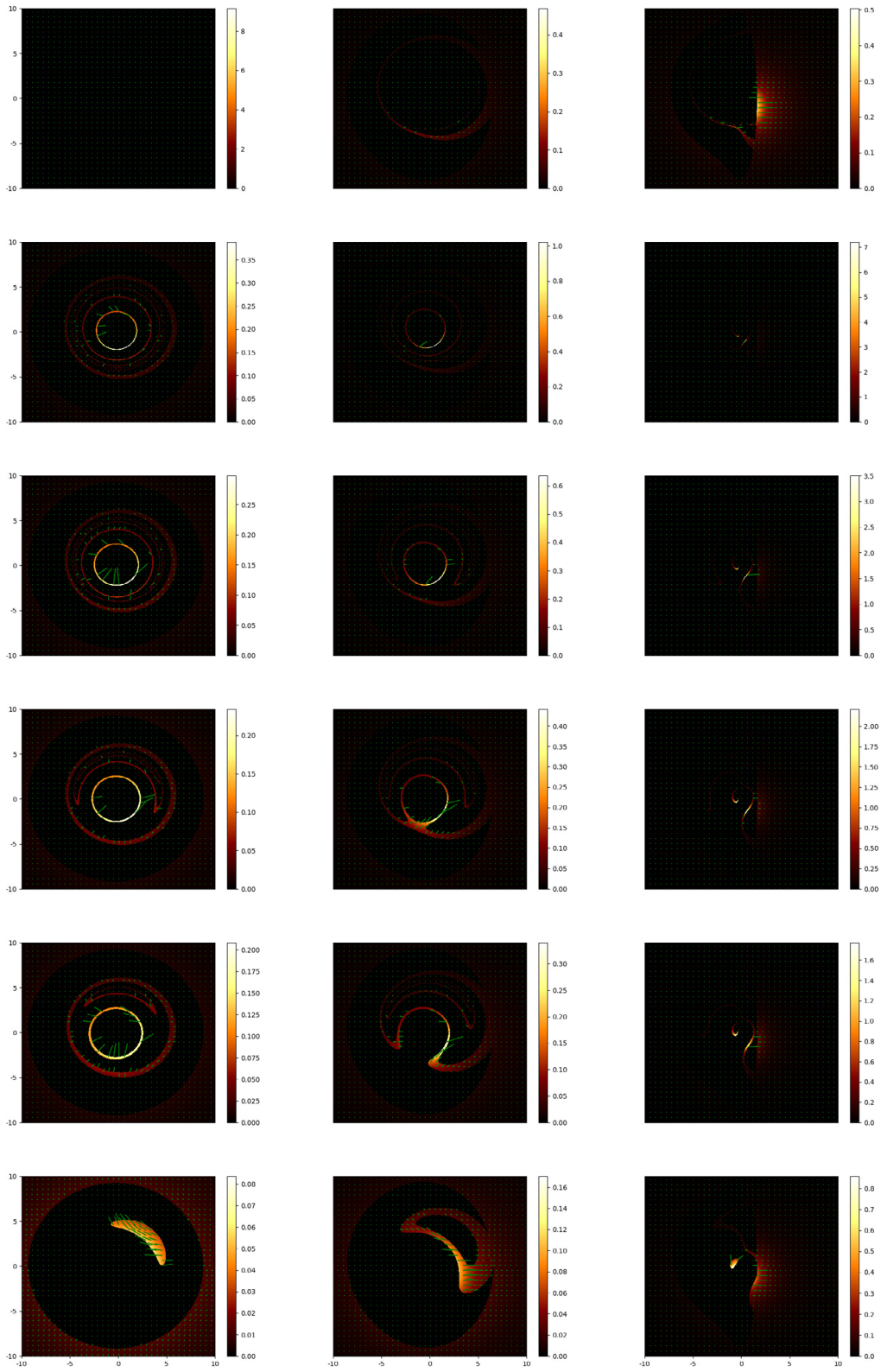

Fig. 2. Map of total linear polarization (shown in color) LP for the initial toroidal distribution of magnetic field around a black hole and wormhole. From left to right, inclination angles are $i = 17^\circ, 45^\circ, 80^\circ$. From top to bottom, magnetic charge is $b = 0, 0.3, 0.5, 0.7, 0.9, 2.0$. Map scale to -10Gm/c^3 to 10Gm/c^3

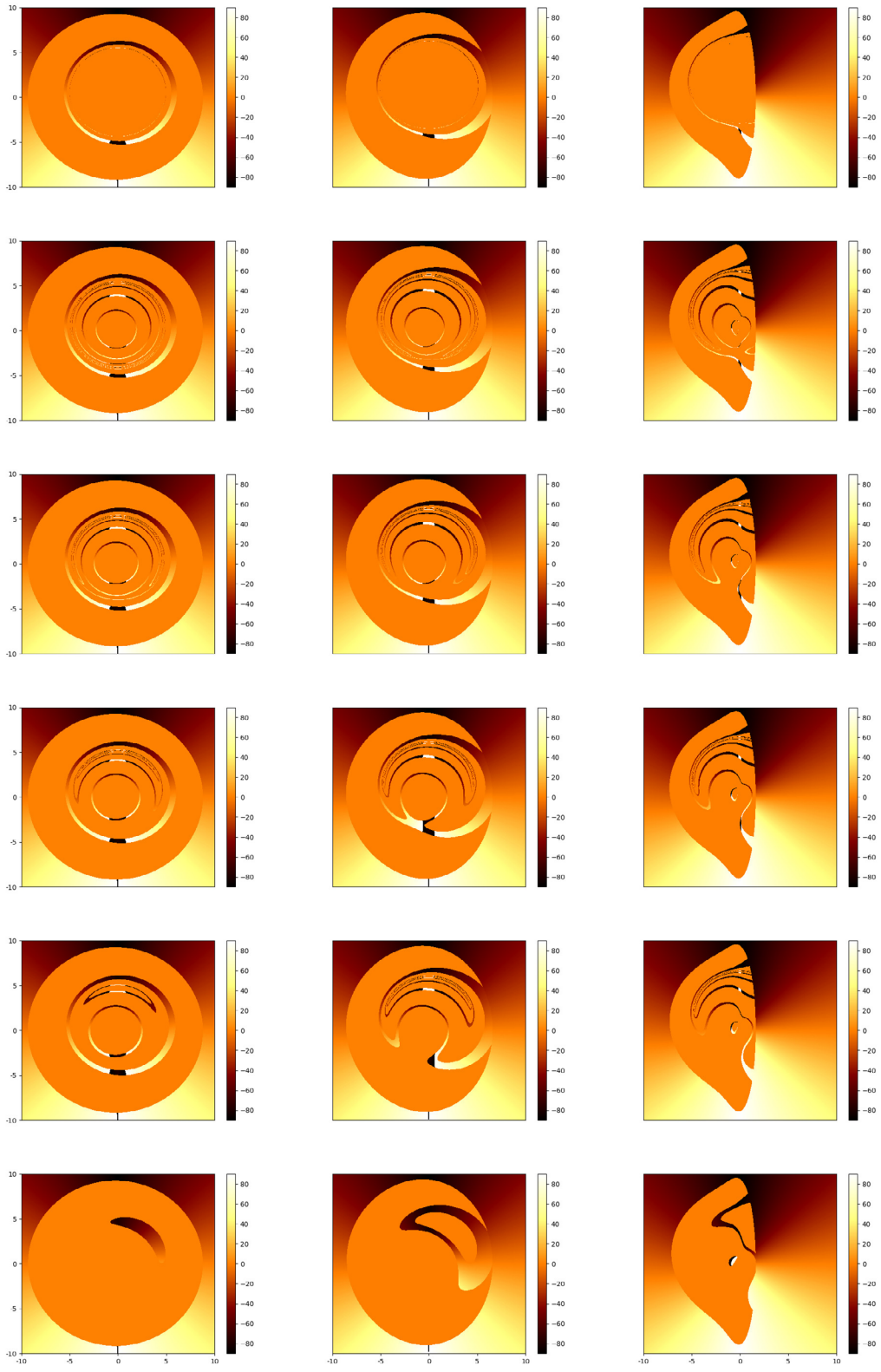

Fig. 3. Map of electric vector position angle (shown in color) for the initial radial distribution of magnetic field around a black hole or wormhole. From left to right, inclination angles are $i = 17^\circ, 45^\circ, 80^\circ$. From top to bottom, magnetic charge is $b = 0, 0.3, 0.5, 0.7, 0.9, 2.0$. Map scale to -10Gm/c^3 to 10Gm/c^3

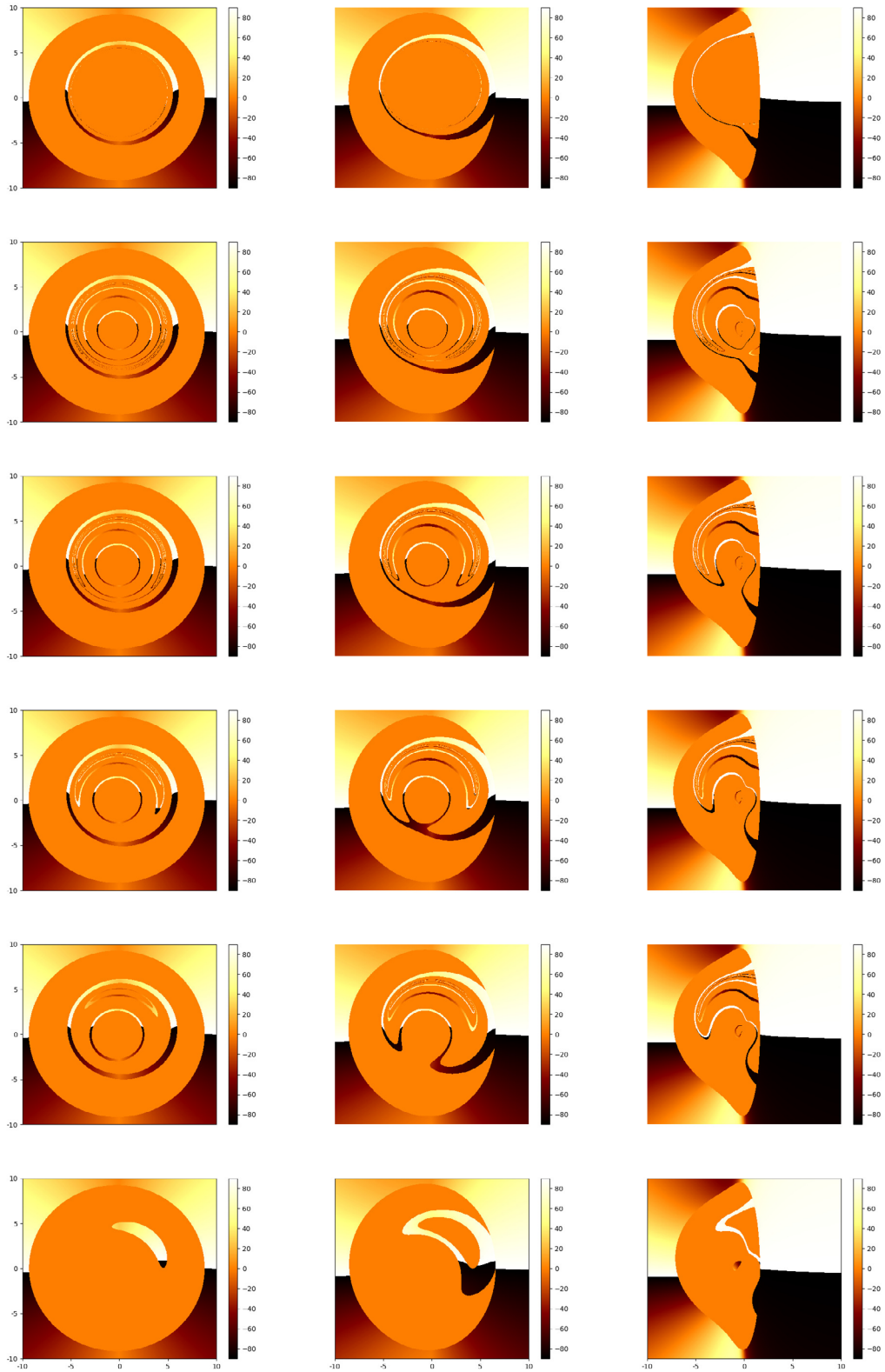

Fig. 4. Map of electric vector position angle (shown in color) for the initial toroidal distribution of magnetic field around a black hole or wormhole. From left to right, inclination angles are $i = 17^\circ, 45^\circ, 80^\circ$. From top to bottom, magnetic charge is $b = 0, 0.3, 0.5, 0.7, 0.9, 2.0$. Map scale to -10Gm/c^3 to 10Gm/c^3

positioned at an angle $i = 17^\circ$ to the rotation axis of the black hole or wormhole. When the observer is positioned at an angle $i = 45^\circ$ or $i = 80^\circ$, the angle between the directions of linear polarization for the initial radial and toroidal magnetic fields will increase.

Figures 3 and 4 show maps of the electric vector position angle for the initial distribution of radial and toroidal magnetic fields, respectively. The color indicates the magnitude of the electric vector position angle. The angle varies from -90° to 90°. Comparing the maps of the electric vector position angle, the following conclusions can be drawn. The magnitude of the electric vector position angle for the radial magnetic field in the disk differs by approximately 90° from the corresponding magnitude for the toroidal magnetic field in the disk. Thus, using the maps of electric vector position angle, one can determine the directions of magnetic field in the disk, i.e., reconstruct the magnetic field topology.

Figures 5 and 6 show the dependencies of the absolute value of parameter on the magnetic charge value at different observer inclination angles to the rotation axis of the black hole or wormhole for cases of radial (Fig. 5) and toroidal (Fig. 6) magnetic fields in the disk. The black solid curve corresponds to the case when the observer is positioned at an angle $i = 17^\circ$ to the rotation axis of the black hole or wormhole, the blue dash-dotted curve corresponds to the case when $i = 45^\circ$, and the green dashed curve corresponds to the case when $i = 80^\circ$. The red vertical line defines the boundary between the black hole (left) and wormhole (right). Figures 5 and 6 show that β_2 remains constant for black holes and changes abruptly at the boundary between the black hole and wormhole. For the radial magnetic field in the disk, the absolute value of $|\beta_2|$ for the black hole will be less than for the wormhole. For the toroidal distribution of the magnetic field in the disk, the situation depends on the observer's inclination to the rotation axis of the black hole (wormhole). For inclinations $i = 17^\circ$ and $i = 45^\circ$, the absolute value of $|\beta_2|$ for the black hole will be less than for the wormhole, while for inclination $i = 80^\circ$ – the situation is reversed. Knowing the observer's inclination angle to the source's rotation axis (black hole or wormhole), the magnetic field distribution in the disk, and measuring the absolute value of $|\beta_2|$ linear polarization, one can conclude whether the source is a black hole or a wormhole.

4. CONCLUSION

This work numerically investigated the polarization properties of black holes and wormholes using the Lamy metric as an example. This metric accurately reproduces the Kerr rotating black hole metric for small magnetic charges and a rotating wormhole otherwise. Using the ray-tracing method, maps of linear polarization and electric vector position angle were constructed for both black hole and wormhole cases.

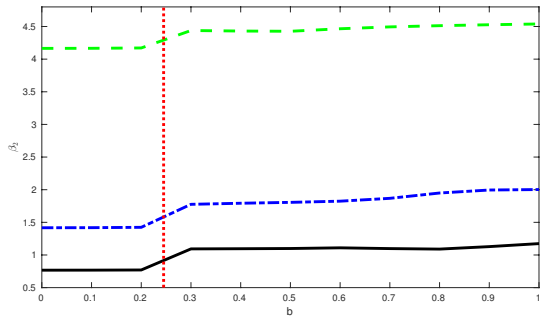

Fig. 5. Dependencies of the absolute value of parameter $|\beta 2|$ on magnetic charge for radial magnetic field in the disk. The solid black curve corresponds to the case when the observer is located at an angle $i = 17^\circ$ to the rotation axis of the black hole or wormhole, the blue dash-dotted curve corresponds to the case $i = 45^\circ$, and the green dashed curve corresponds to the case $i = 80^\circ$. The red vertical dotted line corresponds to the boundary between the black hole (left) and wormhole (right)

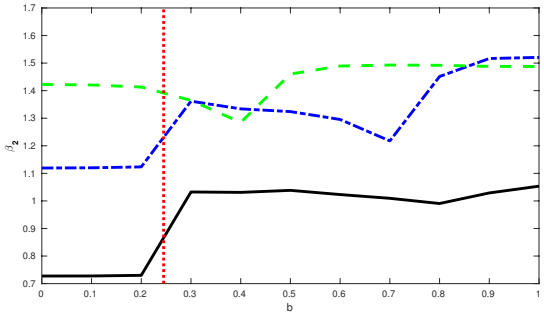

Fig. 6. Dependencies of the absolute value of parameter $|\beta 2|$ on magnetic charge for toroidal magnetic field in the disk. The solid black curve corresponds to the case when the observer is located at an angle $i = 17^\circ$ to the rotation axis of the black hole or wormhole, the blue dash- dotted curve corresponds to the case $i = 45^\circ$, and the green dashed curve corresponds to the case $i = 80^\circ$. The red vertical dotted line corresponds to the boundary between the black hole (left) and wormhole (right)

The photon emission source was set as a thin disk with toroidal or radial magnetic field. Maps of linear polarization and electric vector position angle were constructed. The dependence of the decomposition coefficient $|\beta_2|$ of linear polarization on the magnetic charge magnitude was constructed for different values of observer inclination angles to the rotation axis of the black hole (wormhole) and initial magnetic field distribution. A criterion for distinguishing between a black hole and a wormhole using linear polarization was proposed. By measuring linear polarization, one can reconstruct the magnetic field topology, calculate the decomposition coefficient $|\beta_2|$ and, knowing the inclination, determine whether the source is a black hole or a wormhole.

The study of alternative space-time geometries different from Kerr rotating black hole proves to be particularly timely in connection with the recent results of the Event Horizon Telescope group. The obtained images of galactic centers in M87* and SGR A* have opened new tests of general relativity in strong gravitational fields. The similarity of images of black holes, boson stars, wormholes, and other objects encourages researchers to study alternative geometries in more detail.

APPENDIX

In the Newman-Penrose formalism, four null vectors are introduced ***l, n, m, m****, which satisfy the following conditions [10]: orthogonality condition

$$l \times m = l \times m^* = n \times m = n \times m^* = 0, \tag{16}$$

isotropy condition

$$l \times l = n \times n = m \times m = m^* \times m^* = 0 \tag{17}$$

and normalization condition

$$l \times n = 1, \quad m \times m^* = -1, \tag{18}$$

where the asterisk denotes complex conjugation. By analogy with the Kerr black hole, it can be shown that in the Lamy metric, the following tetrad of vectors satisfies the above relations:

$$l^a = \frac{1}{\Delta}(r^2 + a^2, \Delta, 0, a), \tag{19}$$

$$n^a = \frac{1}{2\Sigma}(r^2 + a^2, -\Delta, 0, a), \tag{20}$$

$$m^a = \frac{1}{\sqrt{2}\bar{r}}\left(ia\sin\theta, 0, 1, \frac{i}{\sin\theta}\right), \tag{21}$$

$$m^{a*} = \frac{1}{\sqrt{2}\bar{r}^*}\left(-ia\sin\theta, 0, 1, \frac{-i}{\sin\theta}\right). \tag{22}$$

For the chosen tetrad of null vectors, the non-zero λ-symbols (see definition of λ-symbols in [10]) are determined by the following relations:

$$\lambda_{(1)(2)(2)} = -\left(\frac{r - M - rM'}{\Sigma} - \frac{r\Delta}{\Sigma^2}\right), \tag{23}$$

$$\lambda_{(1)(3)(2)} = \frac{\sqrt{2}ira\sin\theta}{\bar{r}\Sigma}, \quad \lambda_{(1)(3)(4)} = \frac{1}{\bar{r}^*}, \tag{24}$$

$$\lambda_{(1)(4)(2)} = -\frac{\sqrt{2}ira\sin\theta}{\bar{r}^*\Sigma}, \quad \lambda_{(1)(4)(3)} = \frac{1}{\bar{r}}, \tag{25}$$

$$\lambda_{(2)(1)(3)} = -\frac{\sqrt{2}a^2\sin\theta\cos\theta}{\bar{r}\Sigma}, \tag{26}$$

$$\lambda_{(2)(1)(4)} = -\frac{\sqrt{2}a^2\sin\theta\cos\theta}{\bar{r}^*\Sigma}, \tag{27}$$

$$\lambda_{(2)(3)(4)} = -\frac{\Delta}{2\Sigma\bar{r}^*}, \quad \lambda_{(2)(4)(3)} = -\frac{\Delta}{2\Sigma\bar{r}}, \tag{28}$$

$$\lambda_{(3)(1)(4)} = -\frac{2ia\cos\theta}{\Sigma}, \tag{29}$$

$$\lambda_{(3)(2)(4)} = -\frac{ia\Delta\cos\theta}{\Sigma^2}, \lambda_{(3)(3)(4)} = \frac{r\cos\theta + ia}{\sqrt{2}\sin\theta\bar{r}^2}, \tag{30}$$

$$l_{(3)(4)(4)} = \frac{ia - r\cos\theta}{\sqrt{2}\sin\theta\bar{r}^{*2}}. \quad (31)$$

The spin coefficients (see definition of spin coefficients in [10]) in the Lamy metric are equal to

$$\kappa = \sigma = \nu = \lambda = \varepsilon = 0, \quad (32)$$

$$\mu = -\frac{\Delta}{2\Sigma\bar{r}^{*}}, \quad \pi = \frac{ia\sin\theta}{\sqrt{2}\bar{r}^{*2}}, \quad (33)$$

$$\tau = -\frac{ia\sin\theta}{\sqrt{2}\Sigma}, \quad \rho = -\frac{1}{\bar{r}^{*}}, \quad (34)$$

$$\beta = \frac{\cos\theta}{2\sqrt{2}\sin\theta\bar{r}}, \quad \alpha = \pi - \beta^{*}, \quad (35)$$

$$\gamma = \mu + \frac{r - M - rM'}{2\Sigma}. \quad (36)$$

It can be noted that only the spin coefficient Υ in the Lamy metric differs from the spin coefficient Υ in the Kerr metric.

The Weyl scalar ψ_2 in the Lamy metric is non-zero and equals

$$\Upsilon_2 = -\frac{M}{(r - ia\cos\theta)^3} + rM'\frac{r + ia\cos\theta}{\Sigma^2}. \quad (37)$$

In the case when $\beta = 0$, this expression transitions into the Weyl scalar Ψ_2 in the Kerr metric.

The equations of photon motion in the spacetime of Lamy metric in Boyer-Lindquist coordinates have the same form as in the Kerr metric:

$$\begin{aligned}
\Sigma p^t &= \frac{r^2 + a^2}{\Delta}(r^2 + a^2 - aL) - a^2\sin^2\theta + aL,\\
\Sigma p^r &= \sqrt{(r^2 + a^2 - aL)^2 - \Delta(Q + (a - L)^2)},\\
\Sigma p^\theta &= \sqrt{Q + a^2\cos^2\theta - L^2\frac{\cos^2\theta}{\sin^2\theta}},\\
\Sigma p^\varphi &= \frac{a}{\Delta}(r^2 + a^2 - aL) + \frac{L}{\sin^2\theta} - a.
\end{aligned} \quad (38)$$

Let us recall that the quantity Δ includes parameter (2).

Physical quantities are defined by introducing an orthonormal tetrad. Let us specify an orthonormal tetrad of the form (see [10])

$$\begin{aligned}
e^{\alpha}_{(t)} &= (e^{-\nu}, we^{-\nu}, 0, 0),\\
e^{\alpha}_{(r)} &= (0, e^{-\mu_2}, 0, 0),\\
e^{\alpha}_{(\theta)} &= (0, 0, e^{-\mu_3}, 0),\\
e^{\alpha}_{(f)} &= (0, 0, 0, e^{-\gamma}),
\end{aligned} \quad (39)$$

where the metric coefficients $e^{\nu}, e^{\gamma}, e^{\mu_2}, e^{\mu_3}, w$ are given in the Appendix of paper [8]. The index in parentheses denotes the tetrad index.

We relate quantities in the tetrad basis with quantities in Boyer-Lindquist coordinates through the relations

$$f^{\alpha} = e^{\alpha}_{(a)}f^{(a)}, \quad p^{(a)} = e^{(a)}_{\alpha}p^{\alpha}.$$

In expanded form we have

$$f^t = e^{-\nu}f^{(t)}, \quad p^{(t)} = e^{\nu}p^t, \quad (40)$$

$$f^r = e^{-\mu_2}f^{(r)}, \quad p^{(r)} = e^{\mu_2}p^r, \quad (41)$$

$$f^\theta = e^{-\mu_3}f^{(\theta)}, \quad p^{(\theta)} = e^{\mu_3}p^\theta, \quad (42)$$

$$f^\varphi = e^{-\gamma}f^{(\varphi)} + we^{-\nu}f^{(t)}, \quad p^{(\varphi)} = e^{\gamma}p^\varphi - we^{\gamma}p^t. \quad (43)$$

4-vector of polarization is expressed through the magnetic field in tetrad basis by the formulas

$$f^{(t)} = 0, \quad (44)$$

$$f^{(r)} \mu p^{(\varphi)}B^{(\theta)} - p^{(\theta)}B^{(\varphi)}, \quad (45)$$

$$f^{(\theta)} \mu p^{(r)}B^{(\varphi)} - p^{(\varphi)}B^{(r)}, \quad (46)$$

$$f^{(\varphi)} \mu p^{(\theta)}B^{(r)} - p^{(r)}B^{(\theta)}. \quad (47)$$

Radial field corresponds to the case

$$B^{(r)} = 1, \quad B^{(\theta)} = B^{(\phi)} = 0,$$

toroidal field corresponds to the case

$$B^{(\phi)} = 1, \quad B^{(r)} = B^{(\theta)} = 0.$$

Without loss of generality, we assumed that $f^{(t)} = 0$. By specifying the magnetic field, we can determine the 4-vector of polarization in the radiation source $f^{(a)}$ and using Walker—Penrose constants find the polarization at the observation point. At infinity $r \to \infty$ the values of photon 4-momentum are equal to

$$p^t \to 1, \quad p^r \to 1, \quad p^\phi \to \frac{1}{r^2 \sin^2\theta}, \qquad (48)$$

$$p^\theta \to \frac{\sqrt{\Delta + a^2\cos^2\theta - 1^2 \dfrac{\cos^2\theta}{\sin^2\theta}}}{r^2}, \qquad (49)$$

and 4-vectors of polarization are expressed through Walker—Penrose constants as follows:

$$\sin\theta_0 f^\phi = -\frac{1}{r}\frac{K_1 D_1 + K_2 D_2}{\Delta + (a-1)^2}, \qquad (50)$$

$$f^\theta = \frac{1}{r}\frac{K_1 D_2 - K_2 D_1}{\Delta + (a-1)^2}, \qquad (51)$$

where

$$D_1 = \sqrt{\Delta + a^2\cos^2\theta_0 - 1^2 \frac{\cos^2\theta_0}{\sin^2\theta_0}}, \qquad D_2 = \frac{1}{\sin\theta_0} - a\sin\theta_0. \qquad (52)$$

Electric field is expressed through polarization 4-vectors as follows:

$$E^f = -r\sin\theta_0 f^f, \quad E^\theta = -r f^\theta. \qquad (53)$$

Stokes parameters of linear polarization are defined as

$$Q = E^{\phi 2} - E^{\theta 2}, \quad U = -2E^\phi E^\theta. \qquad (54)$$

To calculate the decomposition coefficient β_m, in the integral

$$b_m = \int_0^{r_{\max}} \int_0^{2\pi} P(r,\phi) e^{-im\phi} r\, dr\, d\phi \qquad (55)$$

we make a change of variables from polar coordinates to Cartesian:

$$x = r\cos\phi, \quad y = r\sin\phi,$$

$$r^2 = x^2 + y^2, \quad \phi = \frac{y}{x}.$$

The Jacobian of transformation equals

$$J = \frac{1}{\sqrt{x^2 + y^2}}.$$

As a result, we obtain

$$b_m = \int_{-10}^{10}\int_{-10}^{10} P(x,y) e^{-im\frac{y}{x}} dxdy =$$

$$= \int_{-10}^{10}\int_{-10}^{10} [Q\cos m\phi + U\sin m\phi + i(U\cos m\phi - Q\sin m\phi)] dxdy, \qquad (56)$$

where integration limits are determined by the sizes of polarization maps (see Fig. 1—4). Coefficient β_2 equals

$$b_2 = \int_{-10}^{10}\int_{-10}^{10} [Q\cos 2\phi + U\sin 2\phi + i(U\cos 2\phi - Q\sin 2\phi)] dxdy, \qquad (57)$$

from which we easily obtain

$$\cos 2\phi = \frac{1 - \tan^2\phi}{1 + \tan^2\phi} = \frac{x^2 - y^2}{x^2 + y^2}, \qquad (58)$$

$$\sin 2\phi = \frac{2\tan\phi}{1 + \tan^2\phi} = \frac{2xy}{x^2 + y^2}. \qquad (59)$$

REFERENCES

1. The Event Horizon Telescope Collaboration et. al. Ap.J.L., 875, L1 (2019).

2. The Event Horizon Telescope Collaboration et. al. Ap.J.L., 930, L12 (2022)

3. S.V. Chernov, Astronomy Reports, 65, 110 (2021).

4. The Event Horizon Telescope Collaboration et. al. Ap.J.L., 910, L12 (2021).

5. The Event Horizon Telescope Collaboration, Astrophys. J. Lett. 910, L13 (2021).

6. F. Lamy, et.al., Classical and Quantum Gravity, 35, 115009 (2018).

7. Z.-Y. Fan, X. Wang, Phys.Rev.D, 94, 124027 (2016).

8. S.V. Chernov, Astronomy Reports, 67, 798 (2023).

9. C.T. Cunningham, J.M. Bardeen, Ap.J. 173, L137 (1972).

10. S. Chandrasekhar, The Mathematical Theory of Black Holes, Moscow, Nauka (1986).

11. D.C.M. Palumbo, G.N. Wong, B.S. Prather, Ap.J. 894, 156 (2020).